Magnetic Resonance Imaging 59 (2019) 105–113

Contents lists available at ScienceDirect

Magnetic Resonance Imaging

journal homepage: www.elsevier.com/locate/mri

Original contribution

# 3 T MR perfusion of solid pancreatic lesions using dynamic contrast-enhanced DISCO sequence: Usefulness of qualitative and quantitative analyses in a pilot study

Francescamaria Donati[a], Piero Boraschi[a,*], Rosa Cervelli[b], Federica Pacciardi[a], Carlo Lombardo[c], Ugo Boggi[c], Fabio Falaschi[a], Davide Caramella[b]

[a] Department of Diagnostic Imaging, Pisa University Hospital, Via Paradisa 2, 56124 Pisa, Italy
[b] Diagnostic and Interventional Radiology, University of Pisa, Via Paradisa 2, 56124 Pisa, Italy
[c] Division of General and Transplant Surgery, University of Pisa, Via Paradisa 2, 56124 Pisa, Italy

ARTICLE INFO

*Keywords:*
Pancreas
Solid pancreatic lesions
MR imaging
Contrast-enhanced MR perfusion
DISCO sequence
Perfusion parameters

ABSTRACT

*Purpose:* To assess the usefulness of qualitative and quantitative analyses of pancreatic focal diseases by using the dynamic contrast-enhanced Differential Subsampling with Cartesian Ordering (DISCO) sequence at 3 T MR device.

*Materials and methods:* Ten patients without pancreatic diseases and twenty-five patients with pathologically confirmed pancreatic focal disease (ductal adenocarcinoma, n = 14; endocrine tumour, n = 8; focal chronic pancreatitis, n = 3), underwent MRI by 3 T-device. Multiphasic contrast-enhanced MR perfusion, consisting of a 3D axial navigator, based free-breathing T1-weighted DISCO sequence, was repeated for 5 min. A dose of 0.1 mL/kg of Gadobutrolo with a 20 mL saline flush was injected at a flow rate of 5 mL/s. Perfusion MRI were processed using a dedicated software package (GeniQ; GE Healthcare), obtaining both a time-signal-intensity curve (TSIC) and perfusion maps for each healthy pancreatic parenchyma and focal disease. The TSIC were grouped into four types according to their shapes and the MR perfusion parameters (Ktrans, Kep, Ve, IAUGC) were calculated.

The one-way analysis of variance and the Student's *t*-test were used to correlate the quantitative and qualitative parameters with the tissue histology.

*Results:* All 10 patients with healthy pancreas presented a TSIC-type 1; TSIC-type 2 was observed in all 14 ductal adenocarcinomas and in one neuroendocrine tumour; TSIC-type 3 was recognized in the remaining 7 neuroendocrine neoplasms; TSIC-type 4 was identified in all 3 focal chronic pancreatitis. All perfusion parameters were significantly different ($p < 0.0001$) for each type of lesion. Furthermore, Ve was also very useful to discriminate between normal and pathological tissues ($p = 0.0005$).

*Conclusion:* Qualitative and quantitative analyses of contrast-enhanced 3 T MR perfusion, using the dynamic contrast-enhanced DISCO sequence, could be considered an interesting tool to improve the diagnosis of focal pancreatic diseases, of solid lesions in particular. Further investigations with prospective larger sample studies are required to confirm these preliminary results.

## 1. Introduction

The MR perfusion can improve the sensitivity and specificity of diagnostic imaging, by providing information about vascular density, permeability, and integrity of the vascular wall. This information can be applied to studies on angiogenesis and biomarkers.

Preliminary studies supported a possible role of MR perfusion in the evaluation of abdominal organs [1–3]. Furthermore, quantitative analysis of perfusion parameters has been considered helpful and an objective tool for the diagnosis of malignant diseases [4,5].

Dynamic contrast-enhanced (DCE) MR perfusion sequence usually lasts several minutes, and each acquisition of the abdominal volume takes from about 15 to 25 s. Not all patients are able to withhold breathing for the whole length of the scan phase, especially the older

* Corresponding author.
*E-mail addresses:* p.boraschi@do.med.unipi.it (P. Boraschi), u.boggi@med.unipi.it (U. Boggi), f.falaschi@ao-pisa.toscana.it (F. Falaschi), davide.caramella@med.unipi.it (D. Caramella).

https://doi.org/10.1016/j.mri.2019.03.001
Received 9 December 2018; Received in revised form 13 February 2019; Accepted 4 March 2019

**Table 1**
MRI protocol.

| Sequence | TR (ms) | TE (ms) | FA (D°) | Multiple *b*-values | Bandwidth (Hz/pixel) | Acceleration (phase/slice) | Slice thickness/spacing | BH/RTr |
|---|---|---|---|---|---|---|---|---|
| 2D-axial and coronal SS-FSE T2w | 1600 | 95 | 90 | | 62.50 | 2/1 | 5/0 | BH |
| 2D-axial FRFSE-propeller T2w | 3500–6000 | 65–90 | 110 | | 36[a] | 2/1 | 5/0 | RTr |
| 2D-axial SPGR-dual echo T1w | 150 | $TE_1$ = 1.3<br>$TE_2$ = 2.5 | 50 | | 166.7 | 2/1 | 5/0 | BH |
| 3D-MRCP FRFSE T2w | 3000–5000 | 600–700 | 90 | | 83.33 | 2/1 | 2.4/−1.2 | RTr |
| 2D-axial SE-EPI diffusion T2w | 4500–7000 | Minimum | 90 | 0<br>150<br>500<br>1000<br>1500 | 250 | 2/1 | 5/0 | RTr |
| 3D axial SPGR-dual echo DISCO T1w | 3.8 | $TE_1$ = 1.1<br>$TE_2$ = 2.2 | 12 | | 200 | 2/2 | 5/−2.5 | Navigator |

TR, repertiotion time; TE, echo time; FA, flip angle; BH, breath holding; RTr, respiratory trigger.
[a] Effect bandwidth.

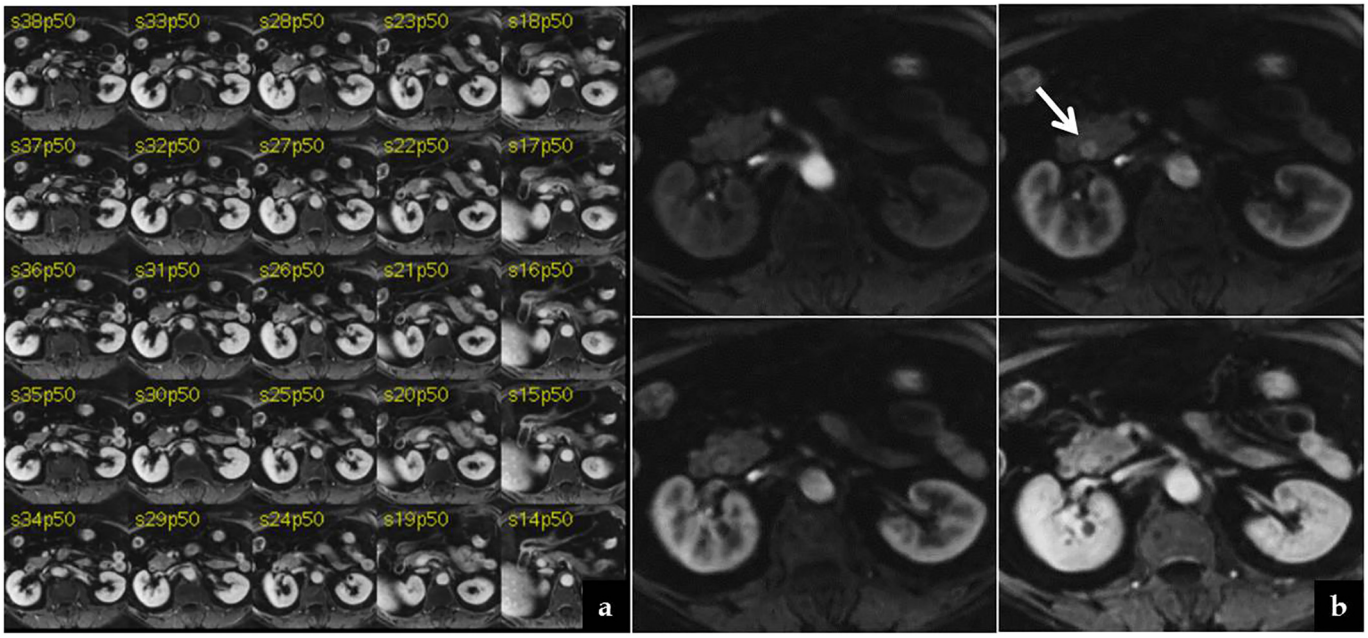


**Fig. 1.** (a,b) Dynamic MR perfusion images. (a) This is a part of the volumetric sets of 40 axial images, obtained during the dynamic MR perfusion acquisition, 120 s after contrast injection. (b) This is the same slab visualized during both first and second arterial, portal-venous and parenchymal phases. Images show the typical contrast-enhancement of a neuroendocrine lesion of the pancreatic head (arrow).

ones. As a consequence, the DCE-MR image quality can be affected by breathing motion artifacts [5]. The use of test bolus DCE-MR imaging, which consists in the administration of a preliminary small test dose of contrast media to determine the optimal time delay, has been proposed to overcome these limitations [6–8]. Huh et al. [5] and Kim et al. [6] reported the reliability timing bolus DCE-MR perfusion parameters to identify the correct diagnosis in solid pancreatic lesions. However, both the sequence technical complexity and the poor image quality compared with multi-phasic dynamic imaging, have limited the widespread use of timing bolus technique.

Recently, Saranathan et al. [9,10] demonstrated the clinical feasibility of Differential Subsampling with Cartesian Ordering (DISCO) sequence, a new high spatial-temporal resolution DCE-MR imaging technique applied to breast and liver anatomical districts.

The advantage of DISCO sequence consists in sampling an elliptically ordered central k-space region every temporal frame as well as in sub-sampling the outer regions in a pseudo-random fashion. By this method the aliasing artifacts from sub-sampling are rendered incoherent. Moreover, a two-point Dixon fat-water reconstruction algorithm allows obtaining fat suppressed images.

Therefore, the purpose of this study was to assess the usefulness of 3 T MR perfusion, using dynamic contrast-enhanced DISCO sequence, of focal pancreatic diseases and solid pancreatic lesions in particular, by performing qualitative and quantitative analyses.

## 2. Material and methods

### 2.1. Study design

This prospective, single-institution study was approved by our institutional review board and a written informed consent was obtained from all patients, after an extensive explanation of the MR exam.

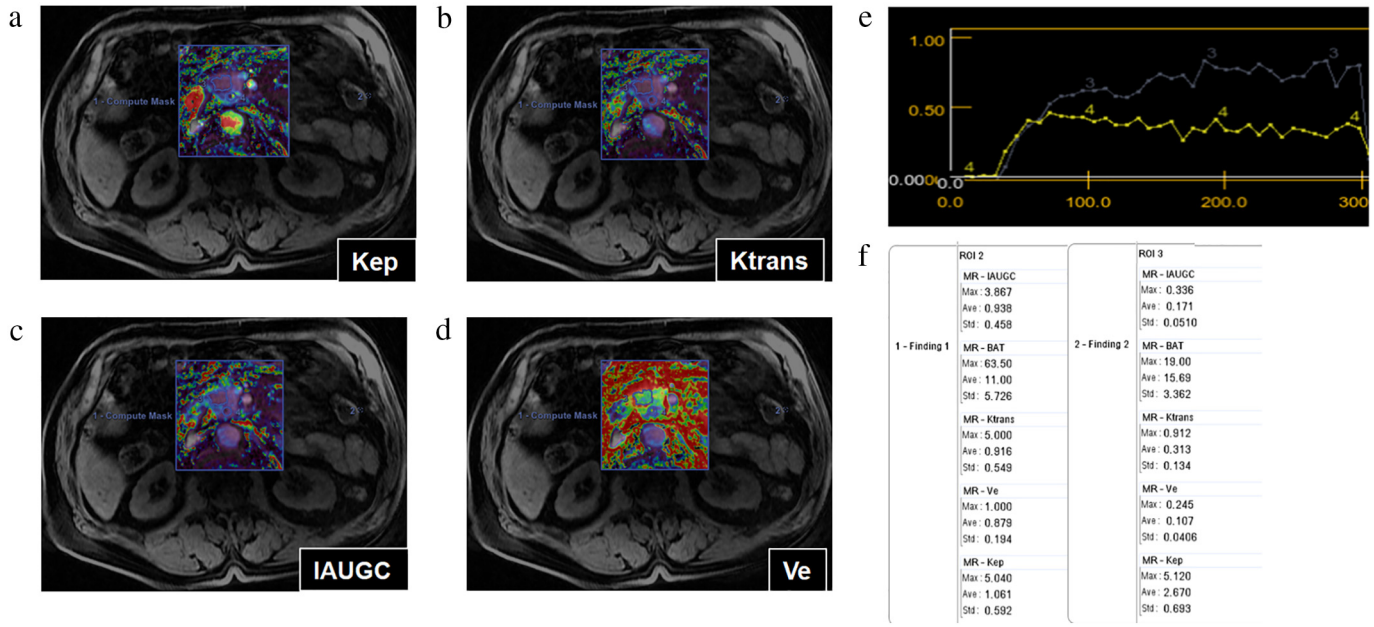


**Fig. 2.** GenIQ parametric view. On the basis of the perfusion maps, a ROI is drawn on both the lesion and the surrounding pancreatic parenchyma, obtaining the perfusion curves and the perfusion parameters value.

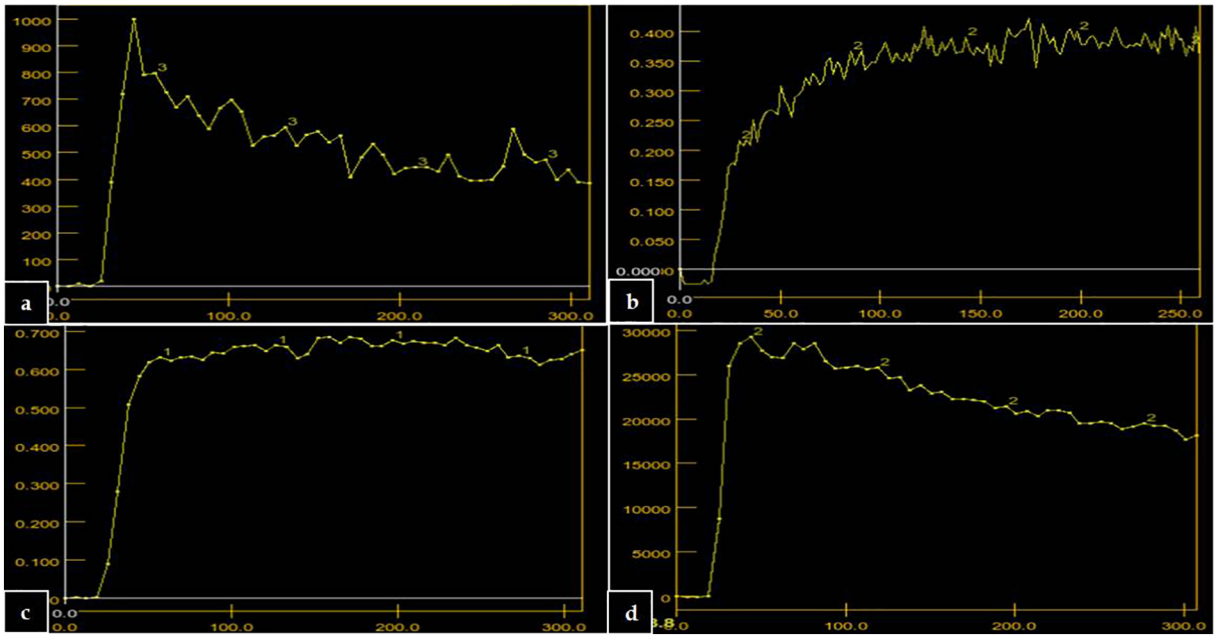


**Fig. 3.** (a–d) Time-signal-intensity curves. Four curve shapes are identified: (a) shape 1, characterized by quick enhancement and quick decay followed by slowly decaying; (b) shape 2, with slow enhancement followed by slow constant enhancement; (c) shape 3, with fast enhancement followed by signal plateau; (d) shape 4 with fast and high enhancement followed by slowly decaying plateau.

### 2.2. Patients

Between April 2016 and April 2017 twenty-five patients with focal pancreatic diseases detected by computed tomography (CT) were prospectively enrolled in our study to be examined by 3 T MR. The inclusion criteria were as follows: (a) CT detection of a focal solid pancreatic disease (the CT exam was performed within 15 days before the enrolment); (b) patients older than 18 years; (c) estimated Glomerular Filtration Rate (eGFR) > 30 mL/min/1.73 $m^2$; (d) absence of absolute or relative contraindications to MR exam; (e) written informed consent signed.

The exclusion criteria were: (a) previous pancreatic surgery; (b) radiation or chemotherapy and/or antiangiogenic therapy within 6 months before the study recruitment; (c) pancreatic gland, free from the targeted focal disease, affected by multiple cysts.

All patients underwent endoscopic ultrasound-guided fine needle biopsy (EUS-FNB) or core biopsy within 1 month after MRI.

To compare the affected patients with a “control group”, ten subjects, who underwent MR examination for focal liver lesions, and found without pancreatic disease and/or symptoms, were enrolled.

### 2.3. MRI technique

All MRI studies were performed by the same 3 T device (GE

**Table 2**
Mean parametric values for each focal pancreatic lesion and for the healthy pancreatic parenchyma.

| | Ktrans mean ± stand. dev. [95% CI] | Ve mean ± stand. dev. [95% CI] | Kep mean ± stand. dev. [95% CI] | IAUGC mean ± stand. dev. [95% CI] |
|---|---|---|---|---|
| Healthy tissue | 0.70 ± 0.09 [0.50–0.90] | 0.20 ± 0.04 [0.17–0.23] | 3.74 ± 0.93 [3.07–4.42] | 0.35 ± 0.08 [0.31–0.40] |
| Focal pancreatitis | 0.58 ± 0.09 [0.21–0.95] | 0.60 ± 0.07 [0.54–0.66] | 0.95 ± 0.07 [−0.29–2.19] | 0.53 ± 0.12 [0.45–0.62] |
| Neuroendocrine tumour | 2.71 ± 0.74 [2.48–2.93] | 0.24 ± 0.08 [0.20–0.27] | 5.96 ± 1.91 [5.20–6.71] | 0.28 ± 0.04 [0.23–0.34] |
| Ductal pancreatic cancer | 0.46 ± 0.05 [0.30–0.64] | 0.34 ± 0.03 [0.31–0.37] | 1.53 ± 0.25 [0.96–2.10] | 0.42 ± 0.07 [0.36–0.49] |

stand. dev., standard deviation.
95% CI, 95% confidence interval.

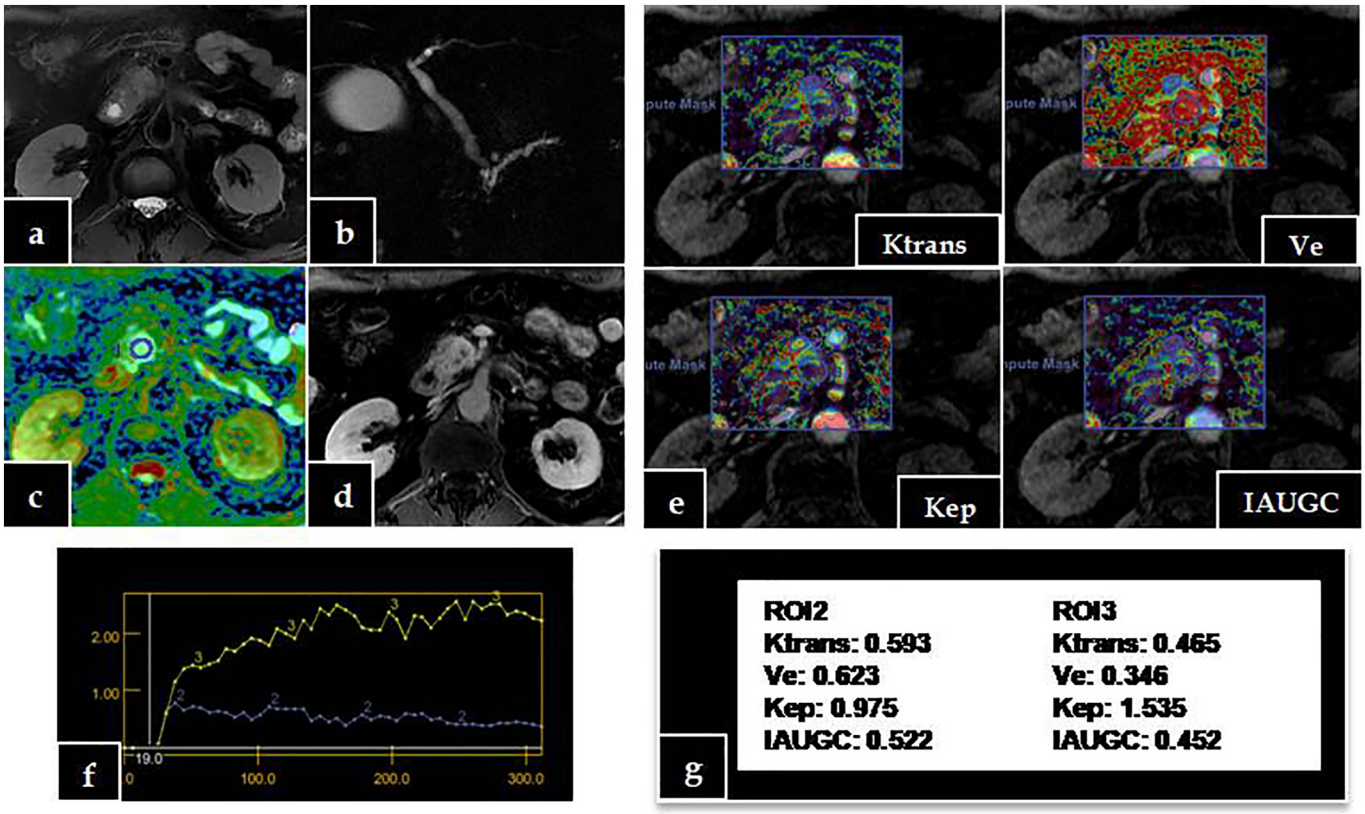


**Fig. 4.** (a–g) Ductal adenocarcinoma. This is a patient with ductal adenocarcinoma at the level of the head. The lesion is identified in T2-weighted (a), MRCP (b), ADC map of DWI (c) and post-contrast T1-weighted (d) images. On the perfusion maps (e) it is well appreciable the differentiation between the lesion and the pancreatic parenchyma, particularly on Ve map. Subsequently, a ROI is placed on the surrounding pancreas (ROI2) and on the lesion (ROI3) obtaining two different curve shapes (f) and also different parametric values (g).

DISCOVERY MR750; GE Healthcare, Milwaukee, Wisconsin, USA) with an eight-channel phased-array body coil. The MR imaging protocol included: 1) axial T1-weighted and axial/coronal T2-weighted images; 2) MR cholangio-pancreatography (MRCP); 3) diffusion weighted MR (DW-MR) sequences. The MR Perfusion was performed using a 3D, axial, navigator based free-breathing, T1-weighted DISCO sequence, which is a high spatial-temporal resolution contrast-enhanced technique. It combines a dual-echo Spoiled Gradient Recalled Echo (SPGR) sequence with Dixon fat-water separation, pseudo-random variable density K-space segmentation and a view sharing reconstruction [9,10]. Free-breathing was compensated by using the navigator echo triggering technique (navigator technique). This technique records the visceral movement and synchronizes the MR images acquired [11]. The MR imaging protocol is summarized in Table 1.

Volumetric sets of 40 axial images (for a total slab thickness of 20 cm) were acquired before contrast media administration. The same volume slab was acquired every 6 s and repeated 50 times during the dynamic post-contrast sequence. The acquisition of the post-contrast first slab started contemporarily with the injection of 0.1 mL/kg of Gadobutrolo (Gadovist, Bayer HealthCare) and 20 mL saline bolus; flow rate of 5 mL/s. The whole length of the sequence was 300 s (Fig. 1).

### 2.4. Image analysis

The overall image quality of the 3D axial navigator based free-breathing T1-weighted DISCO sequence was rated by two abdominal radiologists (with 5 and 15 years of abdominal MRI experience, respectively), using a 4-point scale as follows: score 1 for insufficient quality; score 2 for poor; score 3 for good; score 4 for excellent quality.

Perfusion MR images were processed by both radiologists in

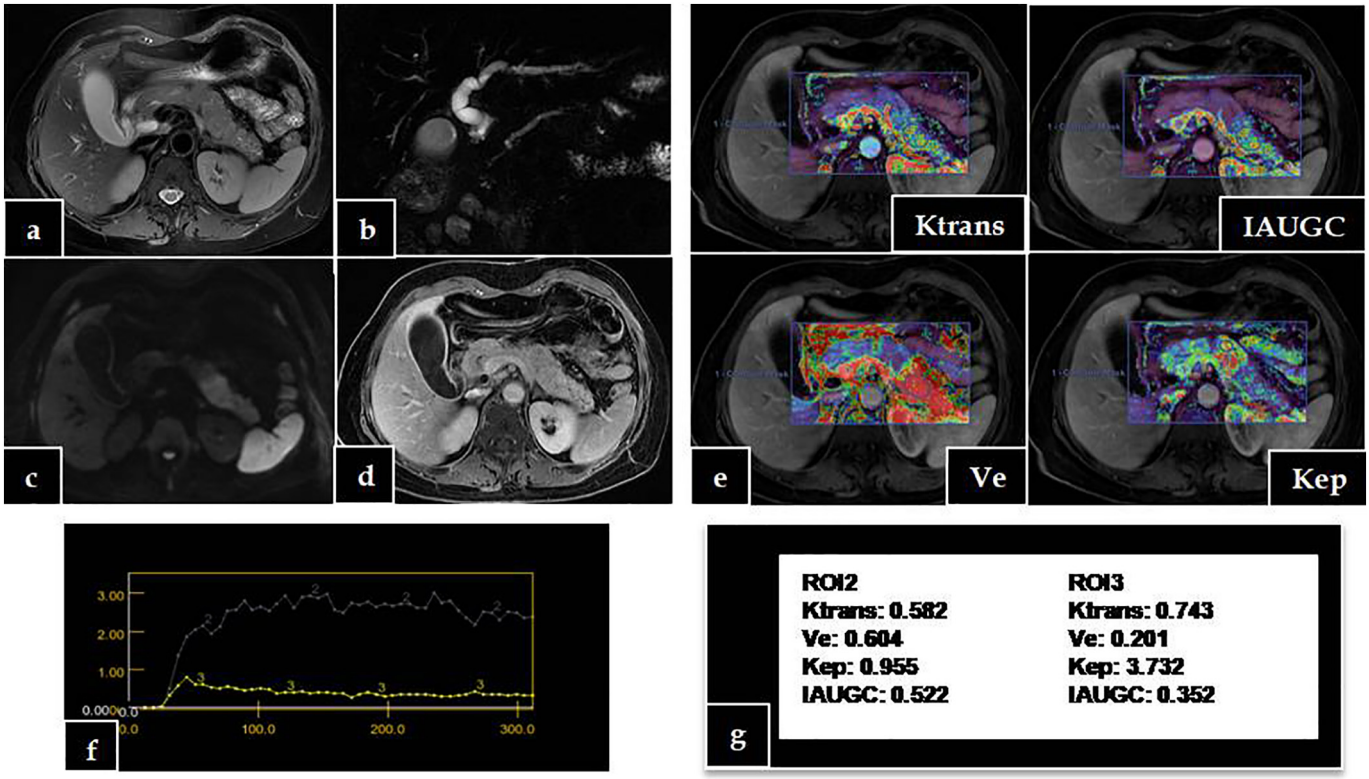


**Fig. 5.** (a–g) Autoimmune pancreatitis. This is a patient with focal autoimmune pancreatitis of the tail with typical findings on T2-weighted (a), MRCP (b), DWI (c) and post-contrast T1-weighted (d) images. In this case on the perfusion maps (e) it is well appreciable the differentiation between the lesion and the pancreatic parenchyma, particularly on Ve map. We placed a ROI on the lesion (ROI2) and on the surrounding pancreas (ROI3) and we obtained two different curve shapes (f); autoimmune pancreatitis' shape curve is like a chronic pancreatitis', however the peak enhancement is higher. Parametric values are different, too (g).

conference, who were blinded to the pathological report of all pancreatic diseases. The perfusion MR analysis was performed by using a dedicated software package “GenIQ”, which is an application on the platform Volume Share 5 running on AW-system (AW VolumeShare 4.7; GE Healthcare, Milwaukee, Wisconsin, USA). It provides automated or semi-automated methods for identifying the optimal Arterial Input Function (AIF).

First, by using GenIQ, the T1 correction factor (3.0 T T1 Pancreas value, relaxation time = 725 ms) was applied to overcome the use of T1 mapping for the quantitative elaboration of the MR perfusion images [12,13]. Then, in presence of motion artifacts, the motion correction factor (available in GenIQ) was used as a post-processing tool. Finally, the T1-signal intensity was converted to gadolinium concentration, in order to obtain both qualitative maps and quantitative parameters (Fig. 2).

On the perfusion maps, regions of interest (ROIs) of 0.5 to 1 cm in diameter, were drawn by two radiologists in conference to obtain both qualitative and quantitative information. The ROIs were drawn on the healthy pancreas in the “control group”, whereas, in the affected patient group, the ROIs were on the focal disease and on the surrounding pancreatic parenchyma.

The qualitative analysis was based on time-signal-intensity curves (TSICs). On the basis of their shape, the TSICs were classified by both radiologists in conference into four types (Fig. 3):

- shape 1, fast enhancement and fast decay, followed by progressive slow decay;
- shape 2, contrast enhancement followed by slow progressive enhancement;
- shape 3, fast enhancement followed by signal plateau;
- shape 4, fast, intense enhancement followed by slow decay, reaching a plateau.

On the basis of TSCIs, the initial area under the gadolinium concentration curve (IAUGC), which includes the perfusion first 60 s, was also calculated.

The quantitative evaluation was based on Tofts' two-compartment pharmacokinetic model [14], the blood flow and the extravascular extracellular space (EES). The following parameters were evaluated:

- Ktrans (volume transfer constant, wash-in)
- Kep (reverse efflux rate constant, wash-out)
- Ve (EES volume fraction).

### 2.5. Statistical analysis

All statistical computations were performed with a dedicated software package (JMP statistical software 7.0, SAS; Cary, NC, USA). Continuous variables were reported as means ± standard deviation (SD); categorical variables were reported as frequencies or percentages. The difference between the values of perfusion parameters obtained by each ROI and the pathological nature of the parenchymal focal disease (neuroendocrine tumour, focal pancreatitis, and ductal adenocarcinoma) or of the healthy tissue was evaluated by the one-way analysis of variance (ANOVA). The quantitative values of perfusion parameters, grouped according to the histological examination, were coupled-compared by Student's *t*-test. Differences were considered statistically significant when the p value was $< 0.05$.

Finally, the correlation between the values of perfusion parameters and the histology was performed by Spearman coefficient.

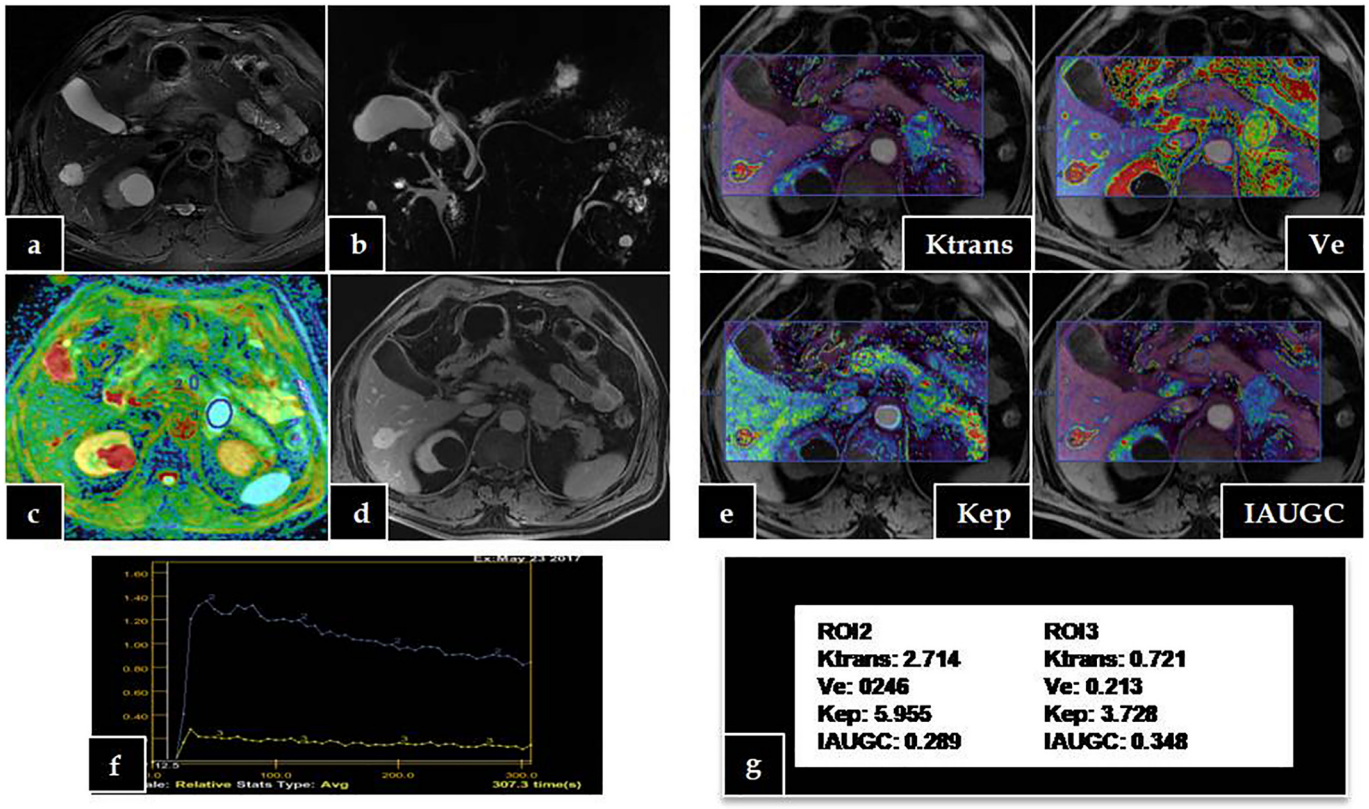


**Fig. 6.** (a–g) Neuroendocrine tumour. This is a patient with neuroendocrine tumour at the level of the tail with a hyperintense hepatic lesion. Both the lesions show the typical appearance on T2-weighted (a), MRCP (b), DWI (c) and post-contrast T1-weighted (d) images. The perfusion imaging well demonstrated the progressive enhancement of the pancreatic lesion and the typical enhancement of the hepatic angioma. On the perfusion maps it is well appreciable the differentiation between the lesion and the pancreatic parenchyma in all maps (e). Subsequently, a ROI is placed on the surrounding pancreas (ROI2) and on the lesion (ROI3) obtaining two different curve shapes (f) and also different parametric values (g). In particular, Ktrans and Kep show the highest values.

**Table 3**
Diamond-graphs of one-way analysis of variance (ANOVA).

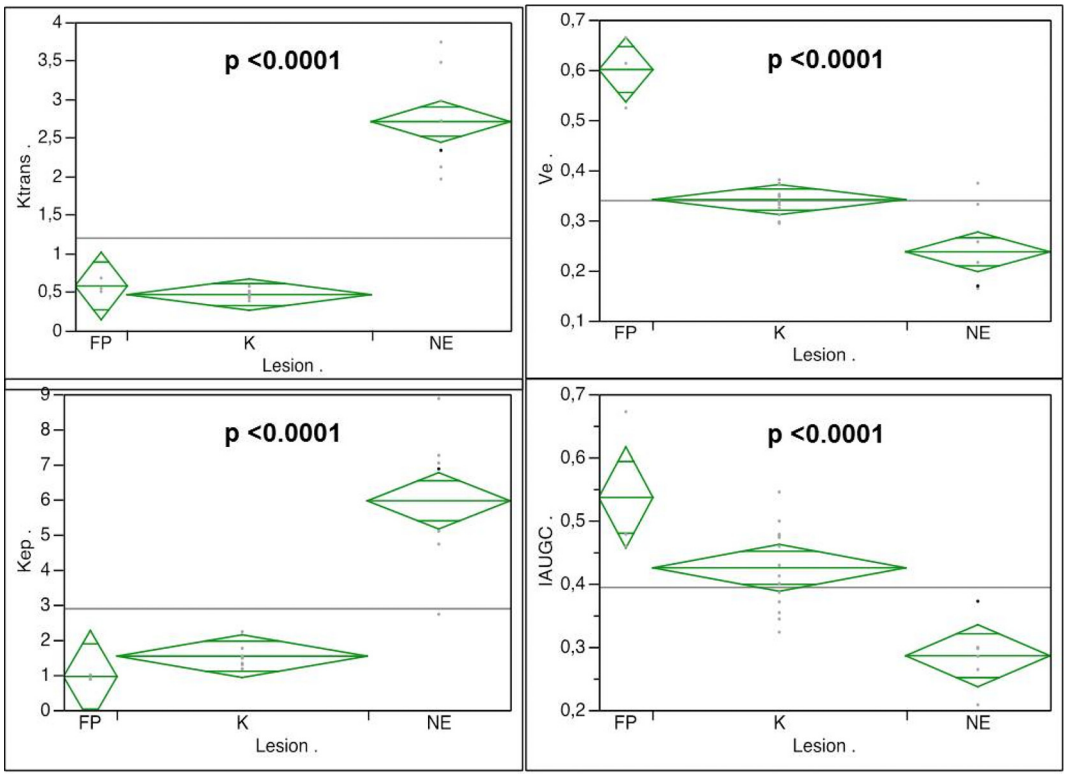

**Table 4**
The Spearman correlation coefficient.

| Variable | Variable by | ρ of Spearman | Prob > IρI |
|---|---|---|---|
| Ve | Ktrans | −0.5330 | 0.0010* |
| Kep | Ktrans | 0.7734 | < 0.0001* |
| Kep | Ve | −0.7125 | < 0.0001* |
| IAUGC | Ktrans | −0.6160 | < 0.0001* |
| IAUGC | Ve | −0.4281 | 0.0103* |
| IAUGC | Kep | −0.6386 | < 0.0001* |
| Normal vs pathological findings | Ktrans | −0.2630 | 0.1269 |
| Normal vs pathological findings | Ve | 0.6077 | 0.0001* |
| Normal vs pathological findings | Kep | −0.3382 | 0.0469* |
| Normal vs pathological findings | IAUGC | 0.1754 | 0.3136 |

* indicates a value statistically significant according to the analysis performed.

## 3. Results

### 3.1. Enrolled patients characteristics

The final histological diagnosis of the focal disease affecting the 25 patients enrolled (16 men and 9 women; age range, 44–83 years; mean age, 64.4 ± 10.3763 years) were the following: ductal adenocarcinoma (n = 14), neuroendocrine tumours (n = 8), and focal chronic pancreatitis (n = 3). According to the NCCN version 2.2017 [15], 9 out of 14 patients were affected by "resectable" adenocarcinoma, whereas the remaining 5 were affected by borderline resectable adenocarcinoma due to the hepatic artery involvement or to the superior mesenteric artery involvement (< 180° of lesion to artery contact). All the patients with borderline resectable lesions were treated by neoadjuvant chemotherapy (FOLFIRINOX) and, then, they underwent surgical resection [16,17]. Only one neuroendocrine tumour was classified as poorly differentiated carcinoma; the remaining 7 were well-differentiated neuroendocrine tumours [18]. Finally, in one out of 3 focal chronic pancreatitis the histology identified autoimmune pancreatitis (type 2).

As to the "control group" (6 men and 4 women; age range, 28–44 years; mean age, 36.1 ± 5.13 years), 7/10 were affected and monitored for hemangioma and 3/10 for focal nodular hyperplasia.

### 3.2. Overall image quality

In all 35 cases, 3D axial navigator based free-breathing, T1-weighted DISCO sequence, covering the whole liver and pancreas with high temporal and spatial resolution, and with high image quality (85,7%, excellent; 14,3%, good), were acquired.

### 3.3. Qualitative analysis results

After image post-processing analysis, all 10 patients with healthy pancreas presented a TSIC-shape 1. The TSIC-shape 2 was observed in all 14 ductal adenocarcinomas and in 1 neuroendocrine tumour; the 3 focal chronic pancreatitis (including the case of autoimmune pancreatitis) showed TSIC-shape 3 curve. Six out of 22 patients affected by solid lesions, showed atrophy of the distal pancreatic gland as a result of the post-obstructive chronic pancreatitis. In all of them, a TSIC-shape 3 curve was obtained when the ROI of the surrounding pancreatic parenchyma was drawn.

Finally, the remaining 7 patients with neuroendocrine tumours showed TSIC-shape 4 curve.

### 3.4. Quantitative analysis results

The perfusion parametric values (IAUGC, Ktrans, Kep and Ve) obtained for each focal pancreatic disease as well as for the healthy pancreatic parenchyma are reported in Table 2. The ANOVA analysis was performed to evaluate the difference of each parametric value (IAUGC, Ktrans, Kep and Ve) grouped on the basis of the assigned histopathologic nature of the focal region assessed. The analysis showed a statistical difference between Ktrans, Ve, Kep and IAUGC values obtained in healthy tissue, ductal adenocarcinoma (Fig. 4), focal chronic pancreatitis (Fig. 5), and neuroendocrine tumour (Fig. 6), respectively (all these statistical computations showed a p value < 0.0001) (Table 3).

Then, the four perfusion parameters were each taken separately and statistically analysed (*t*-Student test) in comparison with two groups at a time, based on the histological examination – healthy pancreatic tissue, ductal adenocarcinoma, neuroendocrine tumour and focal chronic pancreatitis.

By evaluating Ktrans, a statistical difference was found between neuroendocrine tumour and focal pancreatitis, ductal adenocarcinoma and healthy tissue (p < 0.0001); however no statistical difference was obtained between healthy tissue and focal pancreatitis or ductal adenocarcinoma, or between ductal adenocarcinoma and focal pancreatitis.

As to Ve, the focal diseases showed a statistical difference of the value assessed (all with a p value of < 0.0001), except for the neuroendocrine tumour compared with the healthy pancreatic tissue (p = 0.1540); in that case an overlap between the Ve values was recorded.

The Ke resulted statistically different, when each couple of focal diseases was analysed, with the exception of focal pancreatitis versus ductal adenocarcinoma (p = 0.3918). Finally, an overlap of the IAUGC values was recorded only between neuroendocrine tumour and healthy tissue (p = 0.1540).

Statistical correlations were found between the healthy pancreatic tissue or the focal diseases (neuroendocrine tumour, focal chronic pancreatitis and ductal adenocarcinoma) and the perfusion parameters assessed by the ROIs (Spearman correlation coefficient were −0.72, 0.70, −0.66 and 0.45, for Ktrans, Ve, Kep and IAUGC, respectively). A correlation was also found between the healthy or pathological tissue (in the pathological group were included neuroendocrine tumour, focal chronic pancreatitis and ductal adenocarcinoma) and the Ve and Kep values, with a Spearman correlation coefficient of 0.61, and −0.34,

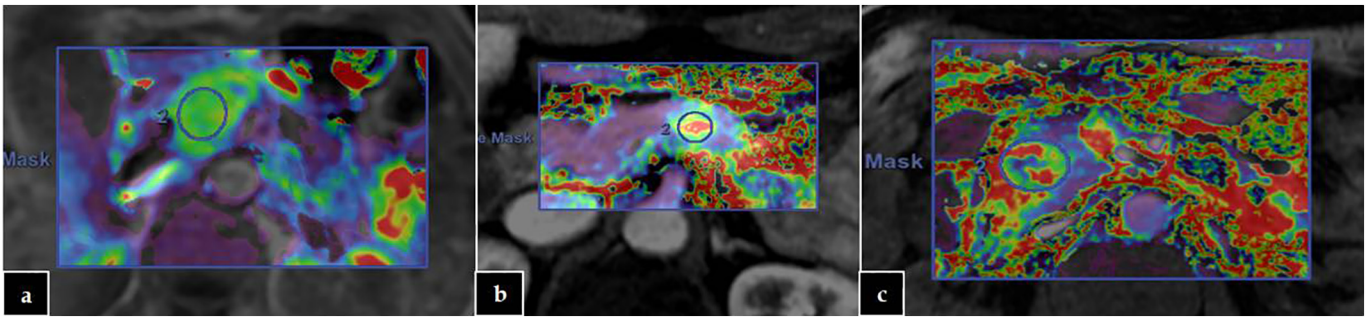


**Fig. 7.** (a–c) Ve perfusion maps. Ve is the most helpful perfusion parameter to discriminate between healthy and pathological tissue in all types of pathologies, for example in focal chronic pancreatitis (a), neuroendocrine tumour (b) and ductal adenocarcinoma (c).

respectively (Table 4).

## 4. Discussion

In our study, DCE-MR imaging by using the DISCO sequence demonstrated clinical feasibility for the perfusion analysis of focal pancreatic diseases. The DISCO sequence, combining a variable density pseudorandom k-space segmentation scheme, view sharing, a 2-point Dixon-based fat-water separation, and 2D parallel imaging using ARC, provides high spatial resolution to characterize lesion morphology and high temporal resolution to accurately characterize contrast behavior. It also provides excellent fat suppression by 3 T device. Furthermore, the DISCO sequence, by applying the navigator gating, avoids artifacts related to breathing-motion, such as image blurring or mismatching [19]. This data were confirmed by our results: the image quality was judged excellent in 85.7% of cases and good in 14.3% of cases.

Differently from previous studies [5–8], which used a small bolus of contrast material to make perfusion (test bolus) followed by the diagnostic DCE-MR sequence, our post-contrast imaging was acquired directly by DISCO. A "standard dose" of gadolinium-based contrast material (0.1 mL/kg of Gadobutrolo) was administered in order to obtain a signal-to-noise ratio comparable with the conventional DCE-MR study. By this technique both time and contrast media were saved, because no further post-contrast sequences were required.

Perfusion qualitative and quantitative assessments were obtained in all cases.

The qualitative assessment, based on the signal intensity per time, showed results in agreement with the ones reported by the Literature [5,6]. All the patients with healthy pancreas presented a TSIC-shape 1. TSIC-shape 2, characterized by contrast enhancement followed by slow progressive enhancement, was observed in all ductal adenocarcinomas and in the only case of poorly differentiated neuroendocrine carcinoma. The remaining 7 patients with neuroendocrine tumour showed TSIC-shape 4 curve, characterized by the typical fast and intense enhancement followed by slow decaying plateau. The different TSIC curve obtained in neuroendocrine tumours can be justified by the histology grade; in fact, the enhancement pattern was different according to the benign, borderline or malignant nature of the neuroendocrine lesion, as demonstrated in previously CT studies [6,20,21]. In particular, when neuroendocrine tumour was malignant, the enhancement pattern corresponded to the ones of the ductal adenocarcinomas.

Finally, all 3 focal chronic pancreatitis showed TSIC-shape 3 curve (including the case of autoimmune pancreatitis), which was characterized by fast enhancement followed by signal plateau. This shape curve was also obtained in 6 cases of post-obstructive chronic pancreatitis, by analysing the surrounding parenchyma in patients with ductal adenocarcinoma. As to the case of autoimmune pancreatitis, the shape of the curve was the same, but the peak enhancement was higher. Although TSIC-shape curves seem to differentiate pancreatic cancer from chronic pancreatitis, there may be enough overlap in the imaging features; so, this differential diagnosis can be often extremely complex [6,22].

For this reason, the quantitative perfusion parameters analysis was also performed.

In our study, the perfusion analysis showed a statistical difference between Ktrans, Ve, Kep and IAUGC values obtained in healthy tissue, neuroendocrine tumour, focal chronic pancreatitis, and ductal adenocarcinoma. However, our results were partially different from those published previously. In particular, the mean perfusion parameter values obtained from healthy pancreatic gland and from each type of focal lesion were different; though, as already reported in the Literature [6,23], the average values of Ktrans and Kep in ductal adenocarcinoma ($0.465\,min^{-1} \pm 0.083$; $1.531\,min^{-1} \pm 0.280$) were significantly lower than those in both healthy pancreas ($0.702\,min^{-1} \pm 0.098$; $3.741\,min^{-1} \pm 0.332$) and focal chronic pancreatitis ($0.577\,min^{-1} \pm 0.180$; $0.951\,min^{-1} \pm 0.606$). On the contrary, Ktrans and Kep averages were higher in neuroendocrine tumour ($2.709\,min^{-1} \pm 0.110$; $5.957\,min^{-1} \pm 0.371$) than in the other focal diseases or healthy pancreatic gland.

The Ktrans and Kep values reflect blood flow (wash-in and wash-out respectively), thus the described results were in agreement with the post-contrast behavior of these primary solid lesions. In fact, the ductal adenocarcinoma is a hypovascular tumour, whereas the well-differentiated neuroendocrine tumour is hypervascularized.

According to the Literature, no statistically significant difference of Ktrans and Kep values was demonstrated between neuroendocrine tumour and neuroendocrine carcinoma [24]. However, in this differential diagnosis, IAUGC could be useful, since the only case of neuroendocrine carcinoma (0.337 mmol/s) did have a higher IAUGC value than that of neuroendocrine tumours ($0.285\,mmol/s \pm 0.025$), comparable to the ductal adenocarcinoma value (0.386–0.463 mmol/s). On the other hand, IAUGC was less useful in the differentiation between focal chronic pancreatitis and ductal adenocarcinoma ($p = 0.019$).

As to Ve, our results have shown that it is the most effective parameter in the differentiation of chronic pancreatitis both from the healthy pancreas and from the other types of focal lesions, in particular in the differentiation from ductal adenocarcinoma (Fig. 7). In fact, the average value of Ve in focal chronic pancreatitis ($0.600\,min^{-1} \pm 0.028$) was significantly higher than in the ductal adenocarcinoma ($0.341\,min^{-1} \pm 0.013$). Despite the low number of chronic pancreatitis in our study group, these data are extremely important, because the differential diagnosis between focal chronic pancreatitis and ductal adenocarcinoma could be sometimes very hard. Finally, Ve is the most useful parameter to differentiate the neoplastic tissue from the healthy parenchyma, showing a Spearman coefficient of 0.6077 ($p < 0.0001$) and this is extremely important in those cases where the differential diagnosis is not clear [25].

Nevertheless, some limitations can be outlined in our study. First, the number of patients was small and heterogeneous for all the types of lesion; moreover the control group was not matched with the group of patients affected by focal pancreatic diseases in order to reduce bias deriving from the population characteristics (age, gender, and so on). The reproducibility and inter-observer variability of perfusion parameters were not evaluated. Finally, there was no reference standard for the perfusion parameters. For these reasons, our results need to be confirmed by a study including a larger series of patients.

## 5. Conclusions

In conclusion, our results suggest that qualitative and quantitative analyses of contrast-enhanced 3 T MR perfusion, using dynamic contrast-enhanced DISCO sequence, could be considered an interesting tool to improve the diagnosis of solid pancreatic lesions. Since DCE-MR DISCO does not require further post-contrast sequences compared to standard MRI examination protocol, this technique could be recommended as an added tool of MR study of the pancreas to characterize focal pancreatic lesions.

## Declarations of interest

None.

## Formatting of funding sources

This research did not receive any specific grant from funding agencies in the public, commercial, or not-for-profit sectors.

## References

[1] Wang L, Zhu HY, Tian JM, Huang SD, Kong LS, Lu JP. Magnetic resonance imaging in determination of myocardial ischemia and viability: comparison with positron emission tomography and single-photon emission computed tomography in a

porcine model. Acta Radiol 2007;48:500–7.
[2] Schraml C, Schwenzer NF, Martirosian P, Claussen CD, Schick F. Perfusion imaging of the pancreas using an arterial spin labeling technique. J Magn Reson Imaging 2008;28:1459–65.
[3] Kim H, Keene KS, Sarver DB, Lee SK, Beasley TM, Morgan DE, et al. Quantitative perfusion- and diffusion-weighted magnetic resonance imaging of gastrointestinal cancers treated with multikinase inhibitors: a pilot study. Gastrointestinal Cancer Research 2014;7:75–81.
[4] Xu QG, Xian JF. Role of quantitative magnetic resonance imaging parameters in the evaluation of treatment response in malignant tumors. Chin Med J (Engl) 2015;128:1128–33.
[5] Huh J, Choi Y, Woo DC, Seo N, Kim B, Lee CK, et al. Feasibility of test-bolus DCE-MRI using CAIPIRINHA-VIBE for the evaluation of pancreatic malignancies. Eur Radiol 2016;26:3949–56.
[6] Kim JH, Lee JM, Park JH, Kim SC, Joo I, Han JK, et al. Solid pancreatic lesions: characterization by using timing bolus dynamic contrast-enhanced MR imaging assessment—a preliminary study. Radiology 2013;266:185–96.
[7] Ueno M, Niwa T, Ohkawa S, Amano A, Masaki T, Miyakawa K, et al. The usefulness of perfusion-weighted magnetic resonance imaging in advanced pancreatic cancer. Pancreas 2009;38:644–8.
[8] Akisik MF, Sandrasegaran K, Bu G, Lin C, Hutchins GD, Chiorean EG. Pancreatic cancer: utility of dynamic contrast-enhanced MR imaging in assessment of anti-angiogenic therapy. Radiology 2010;256:441–9.
[9] Saranathan M, Rettmann DW, Hargreaves BA, Clarke SE, Vasanawala SS. Differential Subsampling with Cartesian Ordering (DISCO): a high spatio-temporal resolution Dixon imaging sequence for multiphasic contrast enhanced abdominal imaging. J Magn Reson Imaging 2012;35:1484–92.
[10] Saranathan M, Rettmann DW, Hargreaves BA, Lipson JA, Daniel BL. A variable spatio-temporal resolution 3D Dixon sequence for rapid dynamic contrast enhanced breast MRI. J Magn Reson Imaging 2014;40:1392–9.
[11] Kim H, Arnoletti PJ, Christein J, Heslin MJ, Posey AJ, Pednekar A, et al. Pancreatic adenocarcinoma: a pilot study of quantitative perfusion and diffusion-weighted breath-hold magnetic resonance imaging. Abdom Imaging 2014;39:744–52.
[12] de Bazelaire CM, Duhamel GD, Rofsky NM, Alsop DC. MR imaging relaxation times of abdominal and pelvic tissues measured in vivo at 3.0 T: preliminary results. Radiology 2004;230:652–9.
[13] Rakow-Penner R, Daniel B, Yu H, Sawyer-Glover A, Glover GH. Relaxation times of breast tissue at 1.5 T and 3 T measured using IDEAL. J Magn Reson Imaging 2006;23:87–91.
[14] Tofts PS, Brix G, Buckley DL, Evelhoch JL, Henderson E, Knopp MV, et al. Estimating kinetic parameters from dynamic contrast-enhanced T(1)-weighted MRI of a diffusable tracer: standardized quantities and symbols. J Magn Reson Imaging 1999;10:223–32.
[15] Tempero MA, Malafa MP, Al-Hawary M, Asbun H, Bain A, Behrman SW, et al. Pancreatic adenocarcinoma, version 2.2017, NCCN clinical practice guidelines in oncology. J Natl Compr Canc Netw 2017;15:1028–61.
[16] Al-Hawary MM, Francis IR, Chari ST, Fishman EK, Hough DM, Lu DS, et al. Pancreatic ductal adenocarcinoma radiology reporting template: consensus statement of the Society of Abdominal Radiology and the American Pancreatic Association. Radiology 2014;270:248–60.
[17] Ramacciato G, Nigri G, Petrucciani N, Pinna AD, Ravaioli M, Jovine E, et al. Pancreatectomy with mesenteric and portal vein resection for borderline resectable pancreatic cancer: multicenter study of 406 patients. Ann Surg Oncol 2016;23:2028–37.
[18] Klimstra DS, Modlin IR, Coppola D, Lloyd RV, Suster S. The pathologic classification of neuroendocrine tumors: a review of nomenclature, grading, and staging systems. Pancreas 2010;39:707–12.
[19] Markl M, Harloff A, Bley TA, Zaitsev M, Jung B, Weigang E, et al. Time-resolved 3D MR velocity mapping at 3 T: improved navigator-gated assessment of vascular anatomy and blood flow. J Magn Reson Imaging 2007;25:824–31.
[20] Chen X, Wang Z. Differences between grades G1 and G2 hypovascular pancreatic neuroendocrine tumors and pancreatic neuroendocrine carcinoma. Radiology 2017;285:331–2.
[21] Belousova E, Karmazanovsky G, Kriger A, Kalinin D, Mannelli D, Glotov A, et al. Contrast-enhanced MDCT in patients with pancreatic neuroendocrine tumours: correlation with histological findings and diagnostic performance in differentiation between tumour grades. Clin Radiol 2017;72:150–8.
[22] Tang MY, Zhang XM, Chen TW, Huang XH. Various diffusion magnetic resonance imaging techniques for pancreatic cancer. World J Radiol 2015;7:424–37.
[23] Luna A, Pahwa S, Bonini C, Alcalá-Mata L, Wright KL, Gulani V. Multiparametric MR imaging in abdominal malignancies. Magn Reson Imaging Clin N Am 2016;24:157–86.
[24] Zhao M, Fu K, Zhang L, Guo W, Wu Q, Bai X, et al. Intravoxel incoherent motion magnetic resonance imaging for breast cancer: a comparison with benign lesions and evaluation of heterogeneity in different tumor regions with prognostic factors and molecular classification. Oncol Lett 2018;16(4):5100–12.
[25] Ma W, Li N, Zhao W, Ren J, Wei M, Yang Y, et al. Apparent diffusion coefficient and dynamic contrast-enhanced magnetic resonance imaging in pancreatic cancer: characteristics and correlation with histopathologic parameters. J Comput Assist Tomogr 2016;40:709–16.